Technetium-99m-Nitroimidazole (BMS181321): A Positive Imaging Agent for Detecting Myocardial Ischemia

Cindy Q.-X. Shi, Albert J. Sinusas, Donald P. Dione, Michael J. Singer, Lawrence H. Young, Eliot N. Heller, Brian D. Rinker, Frans J.Th. Wackers and Barry L. Zaret

Experimental Nuclear Cardiology Laboratory, Division of Cardiovascular Medicine, Department of Internal Medicine, Yale University, School of Medicine, New Haven, Connecticutt

A new technetium-99m-labeled nitroimidazole (BMS181321) has been proposed for positive imaging of myocardial ischemia. **Methods:** An in vivo open-chest canine model of partial coronary occlusion and pacing-induced demand ischemia was used to correlate myocardial retention of BMS181321, following an intravenous injection at peak stress, with regional microsphere blood flow. Postmortem measurements of myocardial BMS181321 activity and flow were correlated with in vivo planar and ex vivo SPECT images. Myocardial and hepatic clearance of BMS181321 was derived from ROI analysis of serial planar images. **Results:** Anaerobic metabolism was documented in the ischemic region by selective venous and arterial sampling for lactate and oxygen consumption. Normalized myocardial BMS181321 activity (165% ± 42% nonischemic) in the central ischemic region (flow < 0.3 ml/min/gm) was significantly greater than activity in normal regions ($p < 0.05$). Quantitative circumferential analysis of SPECT images revealed a comparable increase in myocardial BMS181321 activity in the ischemic region. Sixty minutes after injection of BMS181321, liver activity was 423% of ischemic myocardial activity. **Conclusion:** BMS181321 was preferentially retained in ischemic but viable canine myocardium and was inversely related to regional myocardial blood flow. Although enhanced retention of BMS181321 was detectable by ex vivo SPECT imaging, an unfavorable heart-to-liver ratio was observed with in vivo planar imaging which may limit its use in clinical myocardial imaging.

Key Words: technetium-99m-nitroimidazole; myocardial imaging; ischemia

J Nucl Med 1995; 36:1078–1086

Currently, there are no widely available noninvasive imaging approaches for the direct identification of myocardial ischemia. Since 1973, perfusion scintigraphy during stress has been used to infer regional myocardial ischemia by identification of stress induced flow heterogeneity (*1–3*). Development of flow heterogeneity, however, is not necessarily equivalent to true myocardial ischemia. Myocardial ischemia has also been identified by analysis of myocardial metabolism with [^{11}C]acetate acid (*4*) or [^{11}C]palmitic PET (*5*) and single-photon imaging with radiolabeled free fatty acid analogs (*6*).

More recently, nitroimidazoles have been labeled with the positron emitter ^{18}F in an attempt to directly identify ischemia (*7–11*). This class of nitroimidazole compounds was first developed as selective radiosensitizers of hypoxic cells and used as adjuvants with radiotherapy in the treatment of tumors (*12*). Labeling of nitroimidazoles with PET tracers has permitted the identification of tissue hypoxia or regional ischemia. Studies have shown localization and increased retention of fluoromisonidazole in ischemic brain tissue (*13,14*), in hypoxic isolated myocytes (*9*) and intact ischemic canine myocardium (*7,8,10,11*). The wide application of this approach has been limited in part by the limited availability of PET technology. In addition, fluoromisonidazole has demonstrated fairly slow clearance from the blood (*11*), which may complicate clinical imaging.

The recently developed ^{99m}Tc-labeled nitroimidazole compound, (oxo[[3,3,9,9-tetrmethyl-1-(2-nitro-1H-imidazol-1-yl)-4,8-diazaundecane-2, 10-dione dioxoimato](3-)-N,N′,N″,N‴] technetium) nitroimidazole (BMS181321), may provide an alternative approach for positive imaging of regional myocardial ischemia.

Technetium-99m-nitroimidazole is a lipophilic electron affinic nitroheterocycle which is reduced under hypoxic conditions and is trapped within cells, possibly via covalent bonding to intracellular macromolecules (*15*). In vitro studies suggest that ^{99m}Tc-nitroimidazole is preferentially trapped in and retained by hypoxic but viable cardiac muscle (*16*).

By using an in vivo canine model of partial coronary occlusion and pacing induced demand ischemia, we correlated myocardial retention of ^{99m}Tc-nitroimidazole with regional myocardial blood flow (MBF) in order to evaluate the potential of ^{99m}Tc-nitroimidazole for detection of regional myocardial ischemia. Postmortem measurements of

Received Mar. 18, 1994; revision accepted Jul. 26, 1994

For correspondence or reprints contact: Albert J. Sinusas, MD, Nuclear Cardiology, Yale University School of Medicine, PO Box 3333, 333 Cedar Street, TE-2, New Haven, CT 06510.

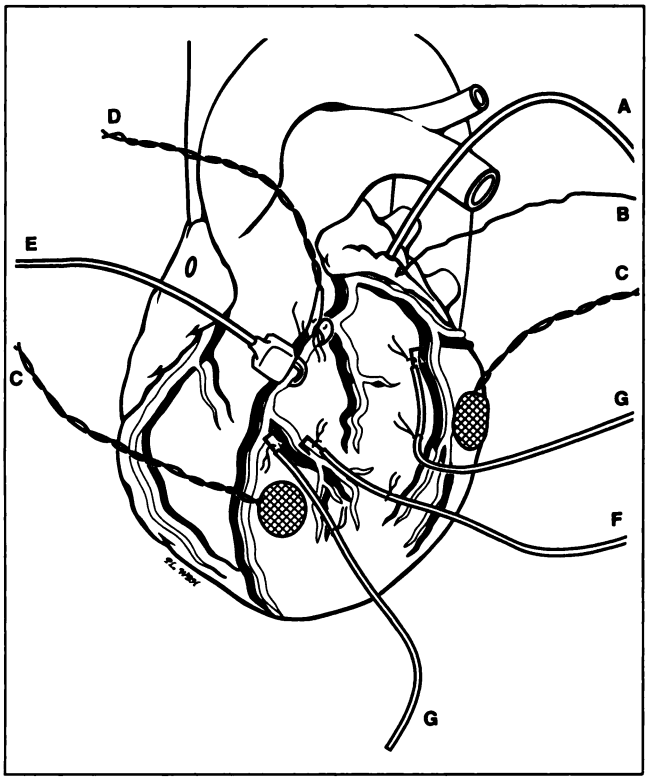

FIGURE 1. Illustration of heart instrumentation. (A) Left atrial catheter, (B) atrial pacing wire, (C) Doppler thickening crystals, (D) Doppler flow probe, (E) hydraulic occluder, (F) distal coronary arterial catheter and (G) coronary venous catheters. The arterial and venous catheters were secured to the heart at two locations after vascular puncture.

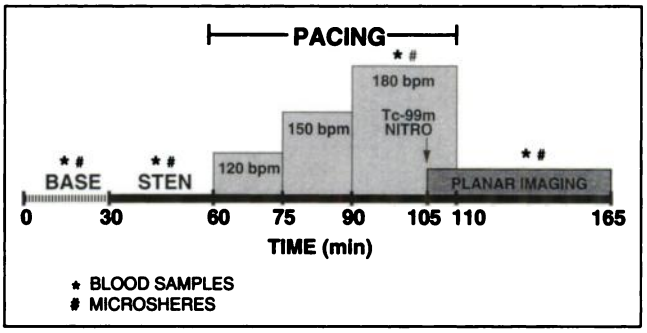

FIGURE 2. After baseline (BASE) measurements, a partial coronary stenosis (STEN) was created and maintained throughout. Blood samples were obtained and microspheres injected at designated times. Dogs were paced in an incremental fashion. Technetium-99m-nitroimidazole was injected at maximum pacing, and serial planar imaging started.

myocardial ^{99m}Tc-nitroimidazole activity and flow were correlated with in vivo ^{99m}Tc-nitroimidazole images.

METHODS

Experiments were performed on fasting adult mongrel dogs with approval of the Yale Animal Care and Use Committee, in compliance with the guiding principles of the American Physiologic Society on research animal use. All dogs were anesthetized with sodium thiamylal (20 mg/kg IV), intubated and mechanically ventilated on a respirator (Boyle Model 50, Harris-Lake Inc.) with a mixture of halothane (0.5%–1.5%), and nitrous oxide and oxygen (N_2O:O_2 = 3:1).

Surgical Preparation

The surgical preparation is illustrated in Figure 1. An electrocardiographic lead was monitored continually. A femoral vein and both femoral arteries were isolated and cannulated for the following: administration of fluids, drugs and ^{99m}Tc-nitroimidazole; pressure monitoring and arterial sampling. Arterial pH, partial pressure of carbon dioxide (PCO_2), and partial pressure of oxygen (PO_2) were measured serially, and the ventilator was adjusted to maintain these parameters within the physiologic range. A left lateral thoracotomy was performed in the fifth intercostal space and the heart suspended in a pericardial cradle. A flared polyethylene catheter was placed in left atrium for the injection of radiolabeled microspheres. A pacing wire was placed in the left atrial appendage. An 8-Fr high fidelity pigtail micromanometer was passed through the carotid artery retrograde into the left ventricle for the measurement of left ventricular pressure and the calculation of dP/dt. The proximal left anterior descending coronary artery (LAD), after the first major diagonal branch, was isolated for placement of a hydraulic occluder. A 20-MHz Doppler flow probe was placed on the LAD just proximal to the occluder. Two 10-MHz Doppler transducers were attached to the epicardium of the left ventricle for measurement of regional myocardial thickening, as previously reported (*17*). One transducer was placed on the anterior left ventricular wall within the central perfusion territory of the LAD, distal to the site of stenosis. The second transducer was positioned on the posterolateral wall of the left ventricle in the distribution of the left circumflex coronary artery.

The distal LAD was cannulated with a catheter designed and constructed in our laboratory. To construct these catheters a 1-in., 25-gauge needle was bent 90° in two locations to form a hook. The blunt end of the needle was inserted into polyethylene tubing (i.d. 0.58 mm, o.d. 0.965 mm, length 10 inches) and secured in place. A 23-gauge blunt needle was inserted into other end of this tubing for connection to a pressurized heparin drip. This apparatus permitted monitoring of distal LAD pressure without compromise of distal flow. The anterior cardiac and obtuse marginal veins were cannulated using the same catheter system for selective venous sampling.

Experimental Protocols

The experimental protocol is summarized in Figure 2. Hemodynamics were monitored continuously and recorded on every 5 min using a data acquisition software package (Dataflow®, Crystal Biotech, Hopkinton, MA). After 30 min of steady-state baseline measurements, a partial stenosis of the LAD was established with the hydraulic occluder. The occluder was adjusted throughout the period of stenosis to maintain the distal LAD pressure at approximately 50% of baseline. After 30 min of low-flow ischemia, the dogs underwent graded atrial pacing at 120, 150 and 180 bpm. Two dogs were not paced at 120 bpm, since baseline heart rate was already increased. Technetium-99m-nitroimidazole (30 mCi) was injected intravenously over 2 min at peak pacing and serial planar gamma camera imaging (15 sec/image) was initiated immediately. Images were acquired for either 30 (n = 2) or 60 min (n = 4). Paired arterial and venous blood samples (1 ml) were collected for the measurement of hemoglobin, O_2 saturation and lactate balance during baseline, stenosis, peak pacing and 30 min after discontinuation of rapid pacing. Regional blood flow was assessed with radiolabeled microspheres in all dogs during base-

line, stenosis, and peak pacing. Three dogs were also injected with radiolabeled microspheres 30 min after discontinuation of rapid pacing. All microspheres were injected immediately following arterial and venous sampling.

Measurement of Myocardial Thickening

Myocardial thickening was assessed in central ischemic and nonischemic regions with pulsed Doppler epicardial transducers. This single-crystal system provides a nontraumatic technique of assessing myocardial thickening. This technique has been validated previously in experimental canine models (*18*). The beginning and end of the systolic interval were determined from the onset of the initial upstroke of left ventricular dP/dt and peak negative dP/dt, respectively. Regional left ventricular wall function was estimated as net systolic thickening. Thickening fraction was calculated by dividing the transmural net systolic thickening by the end diastolic wall thickness, estimated by the range depth.

Measurement of Metabolic Parameters

Oxygen Consumption. Regional oxygen metabolism was assessed by analysis of paired arterial and anterior vein or marginal vein blood obtained for determination of oxygen content. Blood samples were measured immediately for hemoglobin and oxygen saturation using a hemoximeter (Radiometer A/S, Osm3, Copenhagen, Denmark). Average microsphere flow among all segments in both the central ischemic and nonischemic regions were calculated. Regional oxygen consumption (ml O_2/min/100gm) was estimated by multiplying the transmural flow in the region of sampling by the arterial-venous oxygen difference.

Lactate Balance. Whole-blood lactate balance (μmole/min/100 gm) was assessed by analysis of paired arterial and anterior or marginal vein blood. Lactate was measured using an automated lactate oxidase method. Regional lactate consumption was estimated by multiplying transmural blood flow in the region of sampling by the arterial-venous lactate difference.

Preparation of Technetium-99m-Nitroimidazole

Technetium-99m-nitroimidazole was prepared according to previously published methods (*15*). Approximately 30 mCi ^{99m}Tc sodium pertechnetate in 2 ml saline was added to the ligand vial containing BMS 181321. Stannous DTPA was reconstituted with 4 ml of normal saline. A 0.15 ml ($SnCl_2$ 1.88 Ug) aliquot was added to the vial containing ligand and pertechnetate. Radiochemical purity of ^{99m}Tc-nitroimidazole was measured by paper chromatography (TLC), using diethyl ether as a solvent. Chromatographic paper was cut into two pieces and counted in a gamma well counter to determine labeling efficiency. The average percent binding of ^{99m}Tc-nitroimidazole was 92.8% ± 3.8%. Technetium-99m-nitroimidazole was injected within 15 min of preparation.

Image Acquisition and Analysis

In Vivo Planar Imaging. Serial planar images (15 sec/frame) were acquired in the lateral view, using a small field of view gamma camera. Images were acquired with a high-resolution, parallel-hole collimator using a 64 × 64 matrix size. A 20% window was set symmetrically over the 140 keV photopeak of ^{99m}Tc. The camera head was positioned so that the collimator was less than 10 cm from the center of the heart. The heart was displaced from the liver approximately 1 cm with gauze to minimize scattering of liver activity into the heart.

Technetium-99m-nitroimidazole clearance curves were derived from analysis of the dynamic planar imaging sequences obtained. All image analysis was performed off-line on a computer. Four-by-four ROIs were placed over the ventricle and liver. Clearance curves were generated by computing average counts within the ROIs for each frame. In order to compute average curves for all dogs, individual curves were normalized to the value obtained in the terminal 15 sec of each acquisition.

Ex Vivo SPECT Imaging. Hearts were excised at the completion of the protocol and stuffed with saline-soaked gauze. SPECT images were acquired on the excised hearts using a large field of view triple-head rotating gamma camera. Images were acquired with a high-resolution parallel-hole collimator using a 64 × 64 matrix size and 1.42 zoom. A 20% window was set symmetrically over the 140 keV photopeak of ^{99m}Tc. Images (45 sec/frame) were acquired over 360° (6°/stop), using a step and shot method.

Images were reconstructed using standard filtered back projection. A low-pass post reconstruction three-dimensional filter was applied. Reconstructed short axis images (5 mm thick) were transferred to a Sun Sparc-station for quantitative analysis, using a commercial image analysis software package (Analyze®, Mayo Clinic). A circular ROI was drawn around each short-axis slice and divided into eight radial sectors. Quantitative circumferential peak count profiles were generated for each short-axis slice. Apical slices without a clear central cavity were excluded. Basal slices through the membranous septum were also excluded. Weighted averaging of count profiles from the remaining slices (8–11 slices per dog) was performed to generate four short-axis slices corresponding to the postmortem slices. Sectors were visually rotated to optimize registration with the postmortem radial sections (as described below). A maximum anterior-to-posterior image intensity ratio was computed from the most apical short-axis slice using the radial sectors with the highest and lowest counts.

Postmortem Analysis

After SPECT imaging, the hearts were divided into four slices of equal thickness (1–1.5 cm) from base to apex. The slices were incubated in buffered solution of triphenyl tetrazolium chloride (TTC) for 15 min at 38° to detect myocardial necrosis.

Determination of Regional Myocardial Blood Flow and Technetium-99m-Nitroimidazole Activity

Each of the myocardial slices was cut into eight radial sections, which were subdivided into epicardial, midwall and endocardial segments resulting in a total of 96 segments per heart for quantification of myocardial ^{99m}Tc-nitroimidazole activity and blood flow. Myocardial ^{99m}Tc-nitroimidazole activity was measured within 48 hr using a gamma-well autoscintillation counter. The samples were counted again 5 days later for the determination of microsphere flow. Separation of isotopes by energy windows (^{99m}Tc-nitroimidazole, 130–170 keV; ^{51}Cr, 290–360 keV; ^{113}Sn, 361–440 keV; ^{103}Ru, 450–540 keV, ^{95}Nb, 700–810 keV; ^{46}Sc, 811–1160 keV) was performed according to standard methods (*19*), with spill up and spill down correction. Myocardial ^{99m}Tc-nitroimidazole activity was expressed as a percentage of nonischemic as previously reported (*20*) to facilitate comparisons between dogs. Normalized myocardial ^{99m}Tc-nitroimidazole activity was correlated with absolute flow expressed in milliliter per minute per gram. In addition, anterior-to-posterior myocardial ^{99m}Tc-nitroimidazole and flow ratios were computed from the most apical short-axis slice using the radial sectors corresponding with the SPECT image analysis outlined above.

Statistical Analysis

All data are presented as mean ± s.e.m. Comparisons between two groups were made using either a paired or unpaired Student

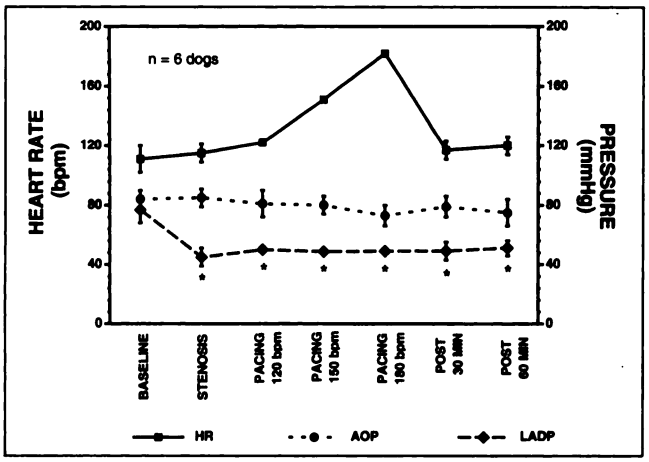

FIGURE 3. Hemodynamics. Serial changes in heart rate (HR), central aortic pressure (AOP) and distal left anterior descending coronary artery pressure (LADP) are shown during baseline, stenosis, atrial pacing (120, 150, and 180 bpm), and 30 and 60 min after discontinuation of pacing. The stenosis produced a significant pressure gradient, which was maintained throughout the protocol. (* $p < 0.05$ versus baseline)

t-test. If multiple comparisons were performed, a Dunnett's multiple comparison test was used. Differences between groups were considered significant at $p < 0.05$ (two-tailed).

RESULTS

Surgical preparation was performed on seven dogs. One dog died during surgery and was excluded. The remaining six dogs completed the experimental protocol. Dogs were killed either 30 (n = 2) or 60 min (n = 4) after ^{99m}Tc-nitroimidazole injection. Two dogs demonstrated a very small infarct (less than 1% of left ventricle) on postmortem TTC staining.

Hemodynamics

Hemodynamic data are summarized in Figure 3. There was no significant change in heart rate or mean aortic pressure with creation of the stenosis. Mean aortic pressure did not change significantly with graded atrial pacing. Thirty minutes after discontinuation of pacing, heart rate and blood pressure had returned to baseline. Distal left anterior descending coronary artery pressure decreased from 77 ± 12 mmHg to 45 ± 9 mmHg during stenosis, representing a 42% reduction in pressure ($p < 0.05$). There was no significant change in the pressure gradient across the stenosis during atrial pacing.

Regional Myocardial Thickening

Changes in thickening fraction in central ischemic and nonischemic region are summarized in Table 1. Partial occlusion of the LAD reduced thickening (% thickening fraction) from 21.3% ± 1.9%, to 7.0% ± 2.2% in the ischemic area. This reduction in thickening fraction represents hypokinesis. As expected regional thickening in the ischemic territory deteriorated further during atrial pacing. The ischemic region became dyskinetic (thickening fraction: −3.2% ± 1.6%) during maximal pacing (180 bpm). Thickening in the remote nonischemic region was also reduced during maximal atrial pacing.

TABLE 1
Thickening Fraction in Central Ischemic and Nonischemic Regions

	Thickening fraction	
	Ischemic (LAD)	Nonischemic (LCX)
Baseline	21.3 ± 1.9	11.5 ± 1.1
Stenosis	7.0 ± 2.2*	13.1 ± 1.6
Pacing 180 bpm	−3.2 ± 1.6*†	5.6 ± 1.3*†
Post 30 min	7.5 ± 3.2*	12.2 ± 1.7

*$p < 0.05$ vs. baseline; †$p < 0.05$ vs. stenosis.

Regional Myocardial Blood Flow

Observed changes in absolute MBF in the central ischemic region and nonischemic region are summarized in Table 2. Flow in ischemic region was also expressed as a percent of nonischemic. Changes in normalized flow in ischemic region are also reported in Table 2. Average transmural resting flow in ischemic region decreased from 1.17 ± 0.29 ml/min/g to 0.66 ± 0.08 ml/min/g with creation of the coronary stenosis. This change, however, did not achieve statistical significance. At peak pacing there was a further reduction in transmural MBF (0.49 ± 0.07 ml/min/g, $p < 0.05$ versus baseline).

Metabolic Parameters

Lactate Balance. At baseline there was lactate consumption in both the perfusion territory of the left anterior descending and left circumflex coronary arteries (Figure 4). Lactate was produced in the central ischemic region following creation of a stenosis of the LAD, which reduced resting flow. During rapid atrial pacing, lactate production was observed in both the ischemic (left anterior descending) and nonischemic (left circumflex) regions.

Oxygen Consumption. Regional oxygen consumption did not change significantly during stenosis of the LAD (Fig. 5). During rapid atrial pacing (180 bpm), there was a significant decrease in oxygen consumption in the ischemic (left anterior descending) region and an increase in oxygen consumption in the control (left circumflex) region. There was evidence of anaerobic metabolism in the perfusion territory of the LAD during maximal atrial pacing at the time of ^{99m}Tc-nitroimidazole injection.

Correlation of Technetium-99m-Nitroimidazole and Regional MBF

Normalized myocardial nitroimidazole activity correlated inversely with absolute myocardial flow. The dogs were killed and then analyzed at 30 and 60 min postinjection separately (Fig. 6). A second order polynomial provided the best fit of these data. A weak relationship between myocardial ^{99m}Tc- nitroimidazole activity and flow was observed for dogs sacrificed at 30 min postinjection, although the relationship improved slightly in those dogs sacrificed at 60 min.

TABLE 2
Microsphere Flow in Central Ischemic Area Expressed in Absolute Flow and as Percentage Nonischemic

	Flow (ml/min/g)			
	Endocardial	Midwall	Epicardial	Transmural
Ischemic — LAD				
Baseline	1.06 ± 0.29	1.11 ± 0.26	1.34 ± 0.31	1.17 ± 0.29
LAD stenosis	0.42 ± 0.11*	0.65 ± 0.09	0.92 ± 0.06	0.66 ± 0.08
Pacing 180 bpm	0.15 ± 0.04*	0.47 ± 0.10	0.84 ± 0.10	0.49 ± 0.07*
Post 30 min	0.53 ± 0.26	0.69 ± 0.23	0.89 ± 0.21	0.71 ± 0.24
Nonischemic — LCX				
Baseline	1.11 ± 0.24	1.02 ± 0.21	0.98 ± 0.21	1.03 ± 0.22
LAD stenosis	0.92 ± 0.09	0.89 ± 0.08	0.86 ± 0.07	0.89 ± 0.08
Pacing 180 bpm	0.88 ± 0.09	1.06 ± 0.11	1.12 ± 0.11	1.02 ± 0.09
Post 30 min	0.81 ± 0.18	0.79 ± 0.17	0.77 ± 0.19	0.79 ± 0.18
	Flow (%nonischemic)			
	Endocardial	Midwall	Epicardial	Transmural
Baseline	90 ± 5	106 ± 3	137 ± 9	110 ± 3
Stenosis	44 ± 9*	74 ± 8*	107 ± 4*	74 ± 6*
Pacing 180 bpm	16 ± 4*†	47 ± 10*†	78 ± 10*†	49 ± 7*†
Post 30 min	59 ± 16*	84 ± 11	117 ± 2	86 ± 9*

*$p < 0.05$ vs. baseline; †$p < 0.05$ vs. stenosis.

Myocardial segments were segregated into five groups based on absolute microsphere flow (severe ischemia, <0.30 ml/min/g; moderate ischemia, 0.30–0.60 ml/min/g; mild ischemia, 0.60–0.90 ml/min/g; nonischemic, 0.90–1.2 ml/min/g; super normal flow, >1.2 ml/min/g). Myocardial ^{99m}Tc-nitroimidazole activity (% nonischemic) in each of these absolute flow ranges is summarized in Figure 7. Normalized myocardial ^{99m}Tc-nitroimidazole activity in the ischemic regions (flow <0.9 ml/min/g) was significantly greater than activity in normal regions.

Technetium-99m-Nitroimidazole Planar Imaging: Distribution and Clearance

Technetium-99m-nitroimidazole activity cleared rapidly from the blood pool, however, it accumulated rapidly in the liver, resulting in a poor target-to-background ratio over the initial 60 min postinjection. Selected frames from the dynamic planar ^{99m}Tc-nitroimidazole imaging sequence are shown for one dog (Fig. 8). Clearance data were derived from serial images acquired in

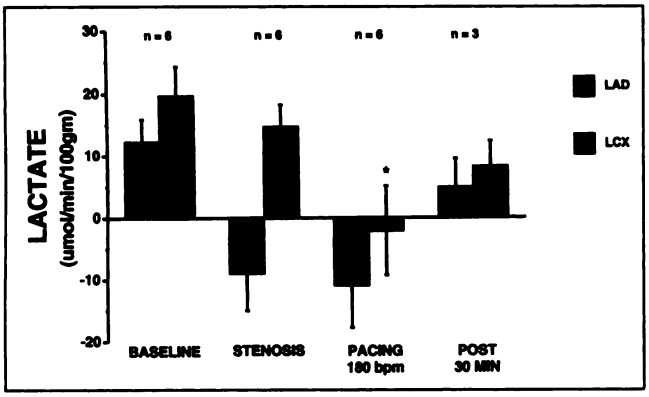

FIGURE 4. Lactate balance is shown for LAD and left circumflex coronary artery (LCX) during baseline, stenosis, peak atrial pacing (pacing 180 min) and 30 min after the discontinuation of pacing (post 30 min). At baseline, there was lactate consumption in both the LAD and LCX regions. Lactate was produced during LAD stenosis. Lactate production occurred in both the ischemic (LAD) and nonischemic (LCX) regions with rapid atrial pacing (* $p < 0.05$ versus baseline).

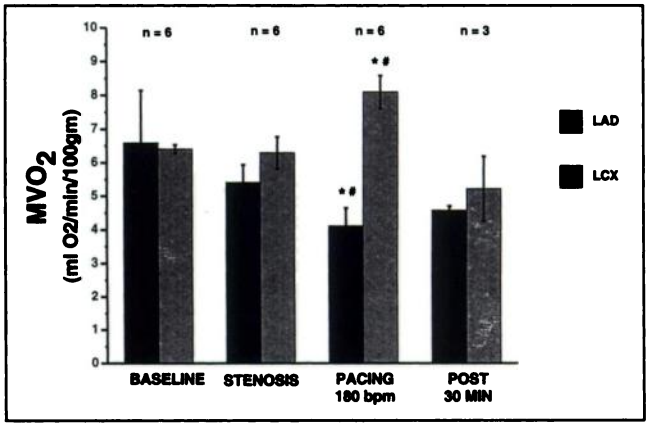

FIGURE 5. Oxygen consumption (MVO_2) for LAD and LCX during baseline, stenosis, peak atrial pacing (pacing 180 min) and 30 min after discontinuation of pacing (post 30 min). There was a significant decrease in oxygen consumption with atrial pacing (180 bpm) in the ischemic (LAD) region at the time of ^{99m}Tc-nitroimidazole injection. Oxygen consumption increased in the control (LCX) region during pacing (* $p < 0.05$ versus baseline, # $p < 0.05$ versus stenosis).

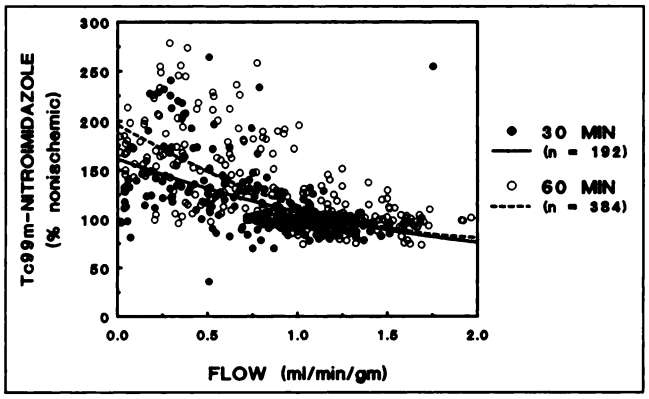

FIGURE 6. Correlation of relative myocardial ^{99m}Tc-nitroimidazole activity (% nonischemic) and absolute regional MBF (ml/min/gm). The two dogs killed 30 min after injection of ^{99m}Tc-nitroimidazole (30 min, filled circles) demonstrated increased ^{99m}Tc-nitroimidazole activity in the low flow regions (solid line: $y = 12x^2 - 66x + 162$; n = 192 segments; r = 0.49). The four dogs killed 60 min after injection (60 min, open circles) demonstrated a similar increase in ^{99m}Tc-nitroimidazole activity in the low flow regions (dashed line: $y = 25x^2 - 109x + 197$; n = 384 segments; r = 0.67).

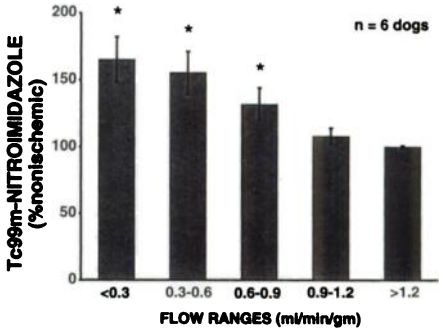

FIGURE 7. Myocardial ^{99m}Tc-nitroimidazole activity (% nonischemic) was evaluated in a series of absolute regional MBF ranges. In segments with flow less than 0.9 ml/min/g, myocardial ^{99m}Tc-nitroimidazole activity was increased relative to activity in normal regions. * $p < 0.05$ versus normal regions [flow 0.9–1.2 ml/min/g].

4 dogs sacrificed 60 min postinjection of ^{99m}Tc-nitroimidazole. Average myocardial and hepatic clearance curves are shown in Figure 9. Ischemic myocardium demonstrated biexponential clearance of ^{99m}Tc-nitroimidazole, while ^{99m}Tc-nitroimidazole accumulated in the liver. At 60 min after injection the activity in the liver was 423% the activity retained in ischemic myocardium on average.

Technetium-99m-Nitroimidazole SPECT Image Quantification

An example of the postmortem ex vivo tomographic short-axis ^{99m}Tc-nitroimidazole images and circumferential quantification are provided in Figure 10. Increased activity was seen in the ischemic anteroseptal region of the four dogs sacrificed 60 min postinjection. Average ^{99m}Tc-nitroimidazole activity observed in the ischemic region on ex vivo SPECT images was 161% ± 22% nonischemic. This was comparable to the increase in ^{99m}Tc-nitroimidazole activity (165% ± 42% nonischemic) measured in the corresponding segments by gamma-well counting.

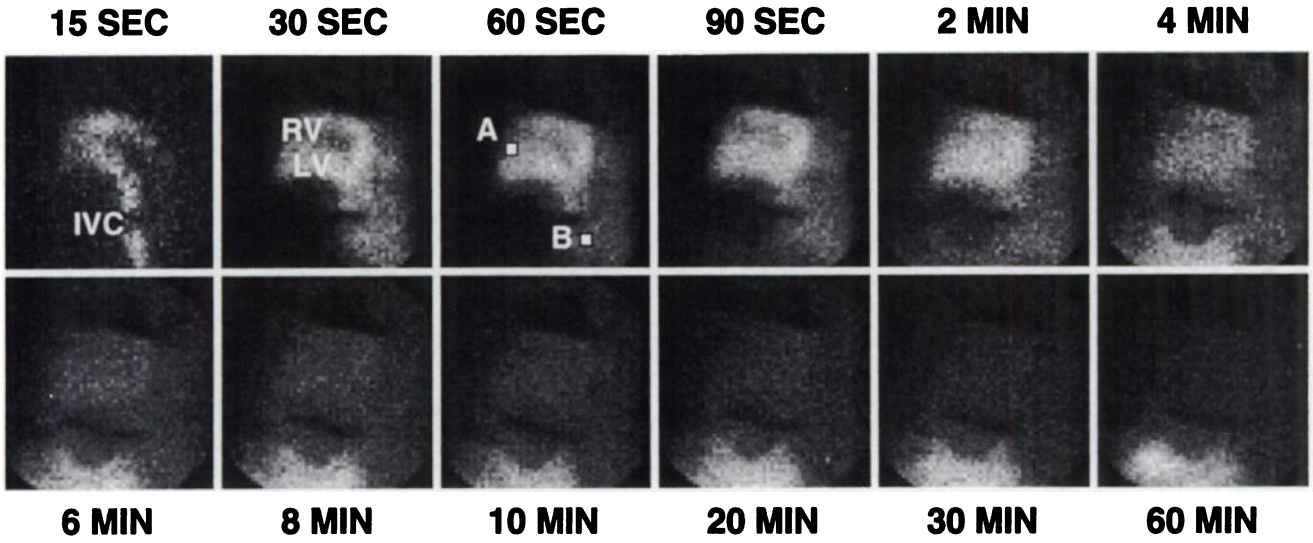

FIGURE 8. Lateral view of serial planar ^{99m}Tc-nitroimidazole images (15 sec/frame). On the 15- and 30-sec images, the inferior vena cava (IVC), right ventricular (RV) and left ventricular (LV) blood pool can be seen. The heart and pericardial cradle were displaced from the liver approximately 1 cm with gauze. Attenuation of background activity from the metal rib spreader can be seen above and below the heart. Technetium-99m-nitroimidazole clearance curves were derived from analysis of complete dynamic planar imaging sequences obtained. Four-by-four ROIs were placed over the myocardium and liver. The myocardial ROI was placed in the central ischemic region of the LAD. Clearance curves were generated by computing average counts within the ROIs for each frame. In this example, activity cleared rapidly from the blood pool, although myocardial-to-background activity ratios were poor. □ = ROI; A = myocardium; B = liver.

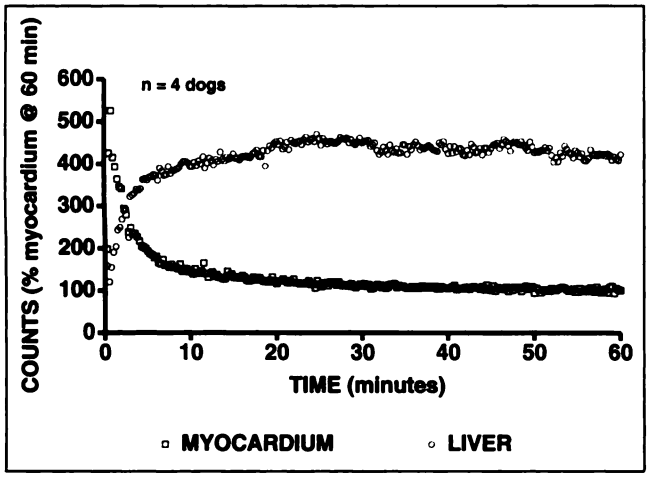

FIGURE 9. Average myocardial and hepatic clearance curves derived from the serial planar images acquired in the four dogs killed 60 min after injection of ^{99m}Tc-nitroimidazole. Both curves were normalized to the myocardial counts in the terminal minute of each serial planar acquisition. Ischemic myocardium demonstrated a biexponential clearance of ^{99m}Tc-nitroimidazole, while the activity accumulated in the liver. At 60 min postinjection, hepatic counts were on average 4.23 times higher than counts measured in the central ischemic region.

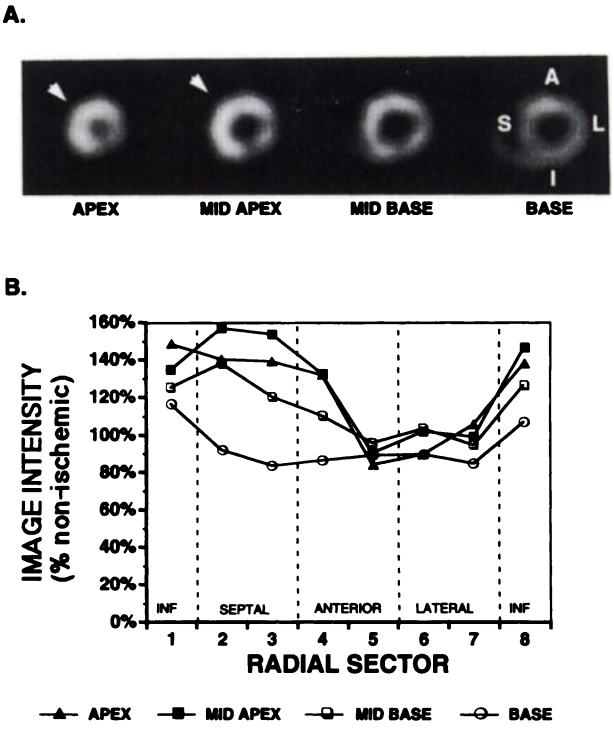

FIGURE 10. Postmortem ex vivo ^{99m}Tc-nitroimidazole tomographic short-axis images (top) and associated circumferential quantitative profiles (bottom). The heart was divided into four short-axis slices from apex to base. Slices are oriented with the anterior wall of the left ventricle superior (A = anterior; L = lateral; I = inferior; S = septum). Increased activity is seen in the anteroseptal region (white arrows). This dog demonstrated a 65% increase in ^{99m}Tc-nitroimidazole activity in the ischemic region.

DISCUSSION

The current study demonstrates that BMS181321 is preferentially retained in ischemic but viable canine myocardium. We produced ischemia in the dog by rapid atrial pacing in the presence of a critical coronary stenosis. Anaerobic metabolism in the ischemic region was verified by reduction in oxygen consumption and lactate production. Myocardial retention of ^{99m}Tc-nitroimidazole was inversely related to regional MBF, as assessed by gamma-well counting. Preferential retention of ^{99m}Tc-nitroimidazole in ischemic myocardium was also detectable by ex vivo tomographic imaging. In vivo planar ^{99m}Tc-nitroimidazole imaging demonstrated relatively low cardiac specificity, which may limit clinical imaging with this agent.

Earlier experimental studies have demonstrated the potential of the positron-emitting radiotracer ^{18}F-misonidazole for the detection of hypoxic myocardium (*8,10,11*). Fluorine-18-misonidazole is a lipophilic tracer which diffuses across the cell membrane. Within the cell the nitro group is thought to undergo reduction by ubiquitous cellular reductase enzymes to form the reactive enzyme radical (*10*). Under normoxic conditions, there is regeneration of the lipophilic parent compound, which freely diffuses back across the cell membrane. Under hypoxic conditions, the reactive nitro anion may bind covalently to intracellular macromolecules or undergo further nitroreduction becoming irreversibly trapped within the cell (*12*).

The exact biochemical mechanism responsible for trapping ^{99m}Tc-nitroimidazole in hypoxic cardiac cells remains unknown, although the retention of ^{99m}Tc-nitroimidazole in ischemic tissue is thought to be similar to other nitroimidazole compounds (*15*). The ^{99m}Tc-nitroimidazole compound was designed to be more lipophilic than fluoromisonidazole. The increased lipophilicity of ^{99m}Tc-nitroimidazole has been recently confirmed (*16*). Increased lipophilicity of ^{99m}Tc-nitroimidazole facilitates diffusion across the cellular membrane. This compound then may undergo nitroreduction in the cytoplasm, which involves enzymatic reduction of the nitro group. When ^{99m}Tc- nitroimidazole was incubated with the enzymes xanthine oxidase and hypoxanthine under anaerobic condition, the nitro group was quantitatively reduced by the enzyme (*15*). In the presence of oxygen, however, ^{99m}Tc-nitroimidazole was not reduced by these enzymes. Rumsey et al. demonstrated that the trapping of ^{99m}Tc-nitroimidazole in myocardium was inversely related to the level of available oxygen and was independent of intracellular energy level or mitochondrial redox in the presence of oxygen (*16*). In an isolated perfused rat heart preparation, ^{99m}Tc-nitroimidazole retention nearly doubled at a perfusate pO_2 of 29 Torr (*21*). In a canine model of LAD stenosis similar to the current study, oxygen pressure decreased below 5 Torr (*22*).

Using an isolated perfused rabbit heart preparation, Dahlberg et al. demonstrated a high initial extraction (Emax) of ^{99m}Tc-nitroimidazole and rapid clearance (*23*). The initial extraction was not affected by either low flow ischemia or hypoxia. In contrast to the previous studies,

Dahlberg et al. demonstrated that while low flow ischemia increased retention (Enet) of ^{99m}Tc-nitroimidazole, hypoxia had no effect on net extraction (*23*).

Our findings of increased myocardial retention of ^{99m}Tc-nitroimidazole in the ischemic region, using an intact canine model of stress induced myocardial ischemia, are concurrent with the previously published in vivo studies using ^{18}F-misonidazole (*10,11*). Our model, although more physiologic then the isolated perfused preparation, can not directly evaluate the effect of hypoxia on ^{99m}Tc-nitroimidazole myocardial kinetics independent of flow.

Experimental Canine Model of Ischemia

We employed an in vivo canine model of partial coronary occlusion and pacing induced demand ischemia. This model was selected to simulate stress-induced ischemia as it may occur in patients with critical coronary artery disease (CAD). We developed and used a catheter system which permits selective sampling of the distal coronary veins, facilitating evaluation of regional myocardial metabolism. Atrial pacing produced regional dysfunction in the central ischemic region associated with a decrease in oxygen consumption and regional lactate production. Atrial pacing in the presence of a stenosis of the LAD also produced regional hypokinesis and altered metabolism in the remote nonischemic left circumflex territory. Recently, Uren et al. demonstrated altered coronary vasodilator reserve and metabolism in myocardium subtended by normal coronary arteries in patients with single vessel CAD (*24*). In this clinical study, atrial pacing in patients with a critical coronary stenosis also produced alteration of regional metabolism in both the ischemic and remote nonischemic regions (*24*).

Clinical Implications

The current study provides evidence for enhanced retention of ^{99m}Tc-nitroimidazole in ischemic myocardium. Retention of ^{99m}Tc-nitroimidazole in the heart was inversely related to flow. A 61% increase in myocardial ^{99m}Tc-nitroimidazole activity in the ischemic region was detectable by ex vivo SPECT imaging within 1 hr of ^{99m}Tc-nitroimidazole injection. The increase in ^{99m}Tc-nitroimidazole myocardial activity in the ischemic region identified by quantitative ex vivo SPECT imaging corresponded to the 65% increase measured by gamma-well counting. This observed heterogeneity of activity should also by detectable by in vivo SPECT imaging.

The relatively low cardiac specificity of ^{99m}Tc-nitroimidazole, however, may limit the feasibility of imaging with this radiotracer clinically. Although blood activity appeared to clear rapidly, we observed significant hepatic activity on in vivo planar images. It should be noted that we placed gauze between the heart and liver, improving our definition of the myocardium on our planar imaging. In spite of this manuever, we observed a relatively poor target-to-background ratio of ^{99m}Tc-nitroimidazole on the planar images.

We also observed a tremendous variability in the uptake of ^{99m}Tc-nitroimidazole relative to flow in the low-flow ranges. This could potentially reduce the characterization from more severely ischemic regions to mild ones. Some of the variability can be related to the relatively large size of the myocardial samples analyzed, which ranged from 0.3 to 1.2 g. Many of the samples contained an admixture of mildly and severely ischemic tissue. Recently, data derived from an in vitro isolated rat heart preparation have in fact demonstrated a sigmoidal relationship between blood oxygen tension and myocardial retention of ^{99m}Tc-nitroimidazole (*25*). This in vitro study suggests that the perfusate oxygen tension must be reduced below a threshold of 60% in order for significant myocardial trapping of ^{99m}Tc-nitroimidazole to occur.

CONCLUSION

The variability and threshold for ^{99m}Tc-nitroimidazole retention we observed, in combination with only a modest increased retention in ischemic regions and unfavorable target-to-background ratios, may impair clinical utilization of ^{99m}Tc-nitroimidazole imaging for detection of regional ischemia. We believe this class of compounds, however, holds promise for positive imaging of ischemia in the heart.

Experimental studies have already supported the possibility of identifying myocardial hypoxia with the positron-emitting compound ^{18}F-fluoromisonidazole noninvasively. The potential of a ^{99m}Tc-labeled nitroimidazole for positive imaging of the heart is tremendous, since single-photon imaging is more widely available. Further investigation of this class of compounds seems warranted.

ACKNOWLEDGMENTS

This research was supported by an aid grant from the Connecticut Affiliate of the American Heart Association and a grant from Bristol-Myers Squibb, Princeton, NJ. Michael McMahon assisted in the planar image analysis and in the preparation of figures.

REFERENCES

1. Zaret BL, Strass HW, Martin ND, Wells HP Jr, Flamm MD. Nonoinvasive regional myocardial perfusion with radioactive potassium. *N Eng J Med* 1973;288:809–1973.
2. Berman DS, Salel AF, Denardo GL, Mason DT. Noninvasive detection of regional myocardial ischemia using rubidium-81 and the scintillation camera: comparison with stress electrocardiography in patients with arteriographically documented coronary stenosis. *Circulation* 1975;52:619–26.
3. Ritchie JL, Hamilton GW, Gould KL, Allen D, Kennedy JW, Hammermeister KE. Myocardial imaging with indium-113m- and ^{99m}Tc-macroaggregated albumin. *Am J Cardiol* 1975;35:380–89.
4. Armbrecht JJ, Buxton DB, Brunken RC, Phelps ME, Schelbert HR. Regional myocardial oxygen consumption determined noninvasively in humans with [1-11C] acetate and dynamic positron tomography. *Circulation* 1989;80:863–872.
5. Bergmann SR, Fox KAA, Geltman EM, Sobel BE. PET of the heart. *Prog Cardiovasc Dis* 1985;28:165–194.
6. Hansen CL, Corbett JR, Pippin JJ, et al. Iodine-123 phenylpentadecanoic acid and SPECT in identifying left ventricular regional metabolic abnormalities in patients with coronary heart disease: comparison with ^{201}Tl myocardial tomography. *J Am Coll Cardiol* 1988;12:78–87.
7. Martin GV, Caldwell JH, Rasey JS, Grunbaum Z, Cerqueira M, Krohn KA. Enhanced binding of the hypoxia cell marker [^{3}H]fluoromisomidazole in ischemic myocardium. *J Nucl Med* 1989;30:194–201.
8. Shelton ME, Dence CS, D-R Hwang, Welch MJ, Bergmann SR. Myocardial

kinetics of fluorine-18 misonidazole: a marker of hypoxia myocardial. *J Nucl Med* 1989;30:351–58.
9. Martin GV, Cerqueira M, Caldwell JH, Rasey JS, Embree L, Krohn KA. Fluromisonidazole: a metabolic marker of myocyte hypoxia. *Circ Res* 1990; 67:240–244.
10. Shelton ME, Dence CS, D-R Hwang, Herrero P, Welch MJ, Bergmann SR. In vivo delineation of myocardial hypoxia during coronary occlusion using florine-18 fluoromisonidazole and PET: a potential approach for identification of jeopardized myocardium. *J Am Coll Cardiol* 1990;16:477–85.
11. Martin GV, Caldwell JH, Graham MM, et al. Noninvasive detection of hypoxic myocardium using fluorine-18-fluoromisonidazole and PET. *J Nucl Med* 1992;33:2202–08.
12. Franko A. Misonidazole and other hypoxia markers: metabolism and applications. *Int J Radiat Oncol Biol Phys* 1986;12:1195–1202.
13. Mathias CJ, Welch MJ, Kilbourn MR, et al. Radiolabeled hypoxic cell sensitizers: tracers for assessment of ischemia. *Life Sci* 1987;41:199–206.
14. Koh W-J, Rasey JS, Evans ML, Grierson JR, Lewellen TK, Graham MM, Krohn KA, Griffin TW. Imaging of hypoxia in human tumor with [F-18]fluromisonidazole. *Int J Radiat Oncol Biol Phys* 1991;22:199–212.
15. Linder KE, Cyr J, Chan Y-W, Raju N, Ramalingam K, Nowotnik DP, Nunn AD. Chemistry of a Tc-PnAO-nitroimidazole complex that localizes in hypoxic tissue. *J Nucl Med* 1992;33(suppl):919.
16. Rumsey WL, Cyr JE, Narra RK. A novel ^{99m}Tc-laveled nitroheterocycle capable of identification of hypoxia in heart. *Biochem Biophys Res Commun* 1993;193:1239–46.
17. Edwards NC, Sinusas AJ, Bergin JD, Watson DD, Ruiz M, Beller GA. Influence of subendocardial ischemia on transmural myocardial function. *Am J Physiol* 1992;262:H568–H576.
18. Hartley CJ, Latson LA, Michael LH, Seidel CL, Lewis RM, Entman ML. Doppler measurement of myocardial thickening with a single epicardial transducer. *Am J Physiol* 1983;245:H1066–H1072.
19. Heymann MA, Payne BD, Hoffman JIE, Rudolph AM. Blood flow measurements with radionuclide-labeled particles. *Prog Cardiovasc Dis* 1977; 20:55–79.
20. Sinusas AJ, Watson DD, Cannon JM, Beller GA. Effect of ischemia and postischemic dysfunction on myocardial uptake of ^{99m}Tc-labeled methoxyisobutyl isonitrile and ^{201}Tl. *J Am Coll Cardiol* 1989;14:1785–1793.
21. Rumsey WL, Patel B, Linder KE. The effect of graded hypoxia on retention of ^{99m}Tc-nitroheterocycle in perfused rat heart. *J Nucl Med* 1994;35:18P.
22. Rumsey WL, Kuczynski B, Patel B, Linder KE. Detecting hypoxia in heart using phosporescence quenching and ^{99m}Tc-nitroimidazoles. *Adv Exp Med Biol* 1994:in press.
23. Dahlberg ST, Gilmore MP, Flood M, Leppo JA. Effect of hypoxia and low flow ischemia on the myocardial extraction of ^{99m}Tc-nitroimidazole. *Circulation* 1993;88(suppl):1339.
24. Uren NG, Marraccini P, Gistri R, De Silva R, Camici PG. Altered coronary vasodilator reserve and metabolism in myocardium subtended by normal arteries in patients with CAD. *J Am Coll Cardiol* 1993;22:650–8.
25. Ng CK, Sinusas AJ, Zaret BL, Soufer R. Kinetic analysis of ^{99m}Tc-labeled nitroimidazole (BMS181321) as a tracer of myocardial hypoxia. *Circulation* 1995:in press.

EDITORIAL

Value of Objective Assessment of New Radiopharmaceuticals

Clinical cardiovascular nuclear medicine and the industries that support and depend on it also depend on the following process:

1. An understanding of the important clinical problems, including scientific, medical and financial issues.
2. Identification of clinical information that is relevant to solving patients' problems.
3. Identification of clinical information that might be supplied uniquely or most efficiently by nuclear medicine methodology.
4. Development of methods to provide new information, including new radiopharmaceuticals, camera/computer systems of hardware and software, and new interventions to alter physiology for imaging of cardiovascular functions.
5. Independent, objective testing of the newly developed methodology.
6. Understanding that problems identified in this testing that will guide development of better final products (continuous quality improvement).
7. Expeditious governmental regulatory/approval process.

The study by Shi et al. (*1*) is an excellent example of a process which advances cardiovascular nuclear medicine. There has always been an interest in detecting myocardial ischemia directly and measuring its extent and severity quantitatively. Basic scientists have measured coronary venous lactate (*2*), tissue concentrations of lactate (*3*), high energy phosphates (*4*) and pH (*5*). Magnetic resonance spectroscopy (MRS) has made real strides in noninvasive imaging of these phenomena (*6*). Certain nitroimidazole compounds have been found to bind, in vitro, selectively to hypoxic cells (*7*). One of these compounds was labeled with ^{18}F for PET imaging (*8*). The fact that an agent binds selectively to hypoxic cells in vitro does not mean that the agent would necessarily be concentrated selectively in ischemic myocardium in vivo because uptake of an agent depends on its delivery by blood flow as well as on extraction from blood to tissue. For example, if the binding of an agent to ischemic cells is twice (2/1) its binding to normal cells (in vitro), but if blood flow is only one-fourth (¼) of normal in the ischemic region (in vivo), then uptake of the agent would be expected to be one-half (½) of normal in the ischemic region ($2/1 \times 1/4 = 1/2$). Such an agent might be imaged most effectively in conjunction with a blood flow tracer where the uptake of the agent relative to blood flow would be twice as great in ischemic as in normal myocardium ($1/2 \div 1/4 = 2/1$).

Because new radiopharmaceutical agents are so important to cardiovascular nuclear medicine, there must be an efficient, rapid process that can assess the potential clinical value of the new agent relative to other agents or modalities. First, in the above example, a perfusion tracer would show up to twofold greater contrast (1/4) compared to a tracer that binds selectively

Received Jan. 23, 1995; accepted Feb. 7, 1995.
For correspondence or reprints contact: Randolph E. Patterson, MD, Carlyle Fraser Heart Center, Emory:Crawford Long Hospital, 550 Peachtree St., NE, Atlanta, GA 30365.